Analytical Biochemistry 410 (2011) 206–213

Contents lists available at ScienceDirect

Analytical Biochemistry

journal homepage: www.elsevier.com/locate/yabio

Escherichia coli-derived von Willebrand factor-A2 domain fluorescence/Förster resonance energy transfer proteins that quantify ADAMTS13 activity

Kannayakanahalli M. Dayananda [a], Shobhit Gogia [a], Sriram Neelamegham [a,b,*]

[a] Department of Chemical and Biological Engineering, State University of New York at Buffalo, Buffalo, NY 14260, USA
[b] New York State Center for Excellence in Bioinformatics and Life Sciences, State University of New York at Buffalo, Buffalo, NY 14260, USA

ARTICLE INFO

Article history:
Received 31 August 2010
Received in revised form 24 November 2010
Accepted 6 December 2010
Available online 10 December 2010

Keywords:
ADAMTS13
Coagulation
Fluorescence
Platelet
Thrombotic thrombocytopenic purpura
VWF

ABSTRACT

The cleavage of the A2 domain of von Willebrand factor (VWF) by the metalloprotease ADAMTS13 regulates VWF size and platelet thrombosis rates. Reduction or inhibition of this enzyme activity leads to thrombotic thrombocytopenic purpura (TTP). We generated a set of novel molecules called VWF-A2 FRET (fluorescence/Förster resonance energy transfer) proteins, where variants of yellow fluorescent protein (Venus) and cyan fluorescent protein (Cerulean) flank either the entire VWF-A2 domain (175 amino acids) or truncated fragments (141, 113, and 77 amino acids) of this domain. These proteins were expressed in *Escherichia coli* in soluble form, and they exhibited FRET properties. Results show that the introduction of Venus/Cerulean itself did not alter the ability of VWF-A2 to undergo ADAMTS13-mediated cleavage. The smallest FRET protein, XS-VWF, detected plasma ADAMTS13 activity down to 10% of normal levels. Tests of acquired and inherited TTP could be completed within 30 min. VWF-A2 conformation changed progressively, and not abruptly, on increasing urea concentrations. Although proteins with 77 and 113 VWF-A2 residues were cleaved in the absence of denaturant, 4 M urea was required for the efficient cleavage of larger constructs. Overall, VWF-A2 FRET proteins can be applied both for the rapid diagnosis of plasma ADAMTS13 activity and as a tool to study VWF-A2 conformation dynamics.

von Willebrand factor (VWF)[1] is a large multimeric glycoprotein found in human circulation. The hemostatic function of this protein increases with protein molecular mass. The size of VWF is regulated by the constitutively active blood metalloprotease ADAMTS13 [1–3], a disintegrin and metalloprotease with thrombospondin type 1 motif 13. This enzyme cleaves the Y1605–M1606 bond, which is constitutively buried within the A2 domain of VWF. The rate of VWF cleavage is enhanced by the application of hydrodynamic/mechanical forces that expose the cleavage site [4]. The binding of VWF to platelet GPIbα [5], endothelial $\alpha_v\beta_3$ [6], and thrombus formation [7,8] further augment this rate of mechanoenzymatic cleavage by enhancing the ability of shear forces to expose the tyrosine–methionine scissile bond. In this regard, VWF binding to cells/surfaces may be important for proteolysis because, at a given shear rate, the force applied on an immobilized protein is 10- to 100-fold more than that in circulation [9,10].

There is currently interest in developing simple and efficient methods to quantify VWF proteolysis rates and ADAMTS13 activity in circulation since such tools can find application in disease diagnosis [11]. Inherited/familial or acquired defects in ADAMTS13 function result in the inefficient cleavage of VWF and the presence of high-molecular-mass VWF in circulation. Whereas inherited defects are associated with severe deficiency of ADAMTS13, acquired disease is typically characterized by the presence of inhibitory autoantibodies. The presence of high-molecular-mass VWF, under these conditions, contributes to the spontaneous binding of platelet receptor GPIbα to VWF via the VWF-A1 domain, platelet activation, aggregation, and microthrombi formation. Such microthrombi can cause vessel occlusion, ischemia, and organ failure, leading to a condition called thrombotic thrombocytopenic purpura (TTP). Thus, accurate and rapid strategies to quantify ADAMTS13 activity can serve as a prognostic marker of TTP.

In the current study, we incorporated into the A2 domain of VWF variants of cyan fluorescent protein (CFP) and yellow fluorescent protein (YFP) that are called Cerulean [12] and Venus [13], respectively. Although 77–175 amino acids of the VWF-A2 domain

* Corresponding author at: Department of Chemical and Biological Engineering, State University of New York at Buffalo, Buffalo, NY 14260, USA. Fax: +1 716 645 3822.
E-mail address: neel@buffalo.edu (S. Neelamegham).

[1] *Abbreviations used:* VWF, von Willebrand factor; TTP, thrombotic thrombocytopenic purpura; CFP, cyan fluorescent protein; YFP, yellow fluorescent protein; GFP, green fluorescent protein; FRET, fluorescence/Förster resonance energy transfer; PCR, polymerase chain reaction; cDNA, complementary DNA; Ven, Venus; Cer, Cerulean; LB, Luria–Bertani; IPTG, isopropyl β-d-thiogalactopyranoside; EDTA, ethylenediaminetetraacetic acid; PPP, platelet poor plasma; SDS–PAGE, Sodium dodecyl sulfate–polyacrylamide gel electrophoresis; NTA, nitrilotriacetic acid; HUS, hemolytic uremic syndrome; ELISA, enzyme-linked immunosorbent assay.

0003-2697/$ - see front matter © 2010 Elsevier Inc. All rights reserved.
doi:10.1016/j.ab.2010.12.005

Table 1
Differences between XS-VWF and FRETS-VWF73.

XS-VWF	FRETS-VWF73
E. coli expression	Chemical synthesis
FRET-based assay	Fluorescence quenching assay
Linear relationship with ADAMTS13 activity	Nonlinear response
Large/77-amino-acid separation between fluorophores	10-amino-acid separation
Excitation = 435 nm (lower plasma autofluorescence)	Excitation = 340–350 nm (high autofluorescence)
Emissions at 485 and 530 nm	Emission = 440–450 nm

separate Cerulean and Venus in the primary sequence of these molecules, the insertion sites of these green fluorescent protein (GFP) variants lie spatially within 2.5 nm in a VWF-A2 crystal structure [14]. Due to this design, the novel family of proteins exhibits fluorescence/Förster resonance energy transfer (FRET) properties. Together, these molecules are called VWF-A2 FRET proteins. The smallest FRET molecule we generated (XS-VWF) detects ADAMTS13 in blood within 5–10 min in the absence of denaturant (K_M = 4 μM), and it can readily detect plasma protease levels down to less than 10% of normal levels. This sensitivity rivals or exceeds the resolution of FRETS-VWF73, another fluorescence-based biosensor of ADAMTS13 activity [15–17]. Other advantages of the VWF-A2 FRET proteins compared with FRETS-VWF73 (Table 1) include the following. First, they are produced in large amounts by *Escherichia coli* in soluble form, unlike FRETS-VWF73 that requires chemical synthesis. The latter synthesis is complicated because the synthetic peptide is long with 73 amino acids. Second, VWF-A2 FRET proteins contain two fluorophores (Venus and Cerulean), unlike FRETS-VWF73 that has one fluorophore and a quencher. Thus, data generated by our molecule can be presented in the form of a FRET ratio (defined in 'Materials and Methods' section). Although the absolute value of this parameter can vary between instruments because detector sensitivity settings at individual wavelengths can be tuned by users, the FRET ratio of the ADAMTS13 cleaved substrate to that of the original intact protein will be approximately 2.75 ± 0.15 regardless of the measuring device and instrument settings. Because FRETS-VWF73 is based on the principles of quenching, however, cleavage measurements vary with instrument settings and assay conditions. Importantly, it is not straightforward to translate the measured fluorescence change to estimate percentage substrate cleavage. Third, due to the large separation between fluorophores in VWF-A2 FRET, unlike FRETS-VWF73 where the fluorophore and quencher are separated by 10 amino acids, our proteins can be applied to study changes in VWF-A2 structure under a variety of conditions in addition to proteolysis. Fourth, the excitation and emission wavelengths used for XS-VWF are higher compared with the FRETS-VWF73 substrate, and this results in lower autofluorescence due to plasma proteins in the former case.

Materials and methods

VWF-A2 FRET constructs

Fusion proteins containing the A2 domain of VWF were expressed in *E. coli*. Many of the proteins were fused to variants of either YFP (Venus and Citrine) or CFP (Cerulean). These fluorophores are monomeric because they incorporate the A206K mutation, and they exhibit higher brightness, lower photobleaching, and higher extinction coefficient and quantum yield when compared with the original CFP and YFP [12,13]. Polymerase chain reaction (PCR) primers used for molecular biology steps are listed in Supplementary Table 1 in the supplementary material.

The plasmids pCS-CG (plasmid no. 12154), pVenus-GalT (11931), pCerulean-VSVG (11913), and pRSET FLII12Pglu-600u (13563) were purchased from Addgene (Cambridge, MA, USA). Initially, pCS-CG was modified by replacing the GFP sequence that it originally contained with the Kozak sequence followed by the VWF signal peptide, *Age*I and *Hpa*I restriction enzyme sites, FLAG epitope, TEV cleavage site, poly 6× histidine tag, and a stop codon. A *Bst*BI enzyme site is present between FLAG and TEV. This vector where the CMV promoter and VWF signal peptide drive protein expression is designated pCSCG-KZK-SS-FLAG-His. Using full-length VWF complementary DNA (cDNA) in pcDNA3.1 (Invitrogen, Carlsbad, CA, USA) as a template [18], the A2 domain of VWF (amino acids 1481–1668) was cloned into pCSCG-KZK-SS-FLAG-His using the *Age*I and *Hpa*I sites for insertion. The resulting plasmid is called pCSCG-A2-FH. Next, the *Kpn*I–*Hin*dIII fragment containing Citrine from pRSET FLII12Pglu-600u was cloned into pUC19. Citrine was amplified in this vector with primers flanked by *Age*I, and it was inserted in the correct orientation at the N terminus of VWF-A2 in pCSCG-A2-FH. The resulting vector is called pCSCG-Citrine-A2-FH, and it was used for mammalian protein expression (results not discussed).

For bacterial expression, the region containing Citrine, VWF-A2, FLAG, TEV site, and polyhistidine from pCSCG-Citrine-A2-FH was amplified by PCR using primers with *Nde*I and *Hin*dIII overhangs, and this was cloned into pRSET-B (Invitrogen). During PCR, sequence encoding for an extra histidine was introduced; thus, all bacterial proteins have a 7× histidine tag. Venus (Ven) from pVenus-GalT with primers containing *Nde*I and *Age*I overhangs also replaced Citrine in pRSET-Citrine-A2-FH to produce pRSET-Ven-A2-FH. Next, Cerulean (Cer) was amplified from pCerulean-VSVG using primers with phosphorylated *Hpa*I compatible overhangs and *Bst*BI, and this was fused at the C terminus of the A2 domain in pRSET-Ven-A2-FH. Insertion of Cerulean resulted in loss of the FLAG epitope. This last vector is designated pRSET-Ven-A2-Cer-H. Based on the VWF-A2 crystal structure (3GXB), regions pertaining to 1496–1670 (L-VWF), 1530–1670 (M-VWF), 1558–1670 (S-VWF), and 1594–1670 (XS-VWF) were amplified by PCR with forward primers containing *Age*I and phosphorylated reverse primers containing *Hpa*I compatible restriction site overhangs. These PCR products that encode for truncated fragments of the full A2 domain were cloned individually into pRSET-Ven-A2-Cer-H. This resulted in a series of products where truncated forms of A2 were flanked by Venus and Cerulean. A2 domain containing Cerulean alone was also created by PCR amplifying A2 (1481–1668) with primers containing *Nde*I and *Hpa*I compatible restriction site overhangs and replacing Venus and L-VWF in the vector pRSET-Ven-(L-VWF)-Cer-H. This product is called pRSET-A2-Cer-H. To generate XS-VWF(AA), we mutated the Y1605–M1606 sequence in XS-VWF (1594–1670) to A1605–A1606. To this end, a mega primer was first generated using a reverse primer containing the YM-to-AA mutation and a forward primer encoding for the start of the XS-VWF sequence. The PCR product was purified using a QIAquick PCR Kit (Qiagen, Valencia, CA, USA), and this was used along with a reverse primer encoding for the 3' section of XS-VWF during the second PCR step. The final PCR product was cloned into pRSET-Ven-(L-VWF)-Cer-H to replace L-VWF. DNA sequencing was performed to verify all plasmid constructs described above.

Expression and purification of VWF-A2 FRET proteins from E. coli

pRSET vectors encoding for VWF-A2 constructs were transformed into *E. coli* BL21 Star or other strains. Single colonies were scaled up to 1 L in Luria–Bertani (LB) broth supplemented with 50 μg/ml ampicillin. Cells were grown to OD_{600} = 0.6 at 37 °C and then induced with 1 mM isopropyl β-D-thiogalactopyranoside (IPTG) for 12 h at 30 °C. Following this, all protein purification steps

described below were performed at 4 °C. First, the cells from 1 L of culture were centrifuged at 2000*g* for 20 min, washed with phosphate-buffered saline, and then resuspended in 10 ml of 20 mM Hepes buffer (pH 7.4) containing 300 mM NaCl, 10 mM imidazole, and ethylenediaminetetraacetic acid (EDTA)-free protease inhibitor cocktail (Roche Diagnostics, Indianapolis, IN, USA). Cells were then lysed by three cycles of freeze–thaw. Lysozyme (10 μg/ml) was added for an additional 30 min to further facilitate lysis. Following this, the genomic DNA was sheared using a Branson sonifier (Danbury, CT, USA). Lysate was separated from the cell debris by centrifuging at 20,000*g* for 30 min. The pellet was discarded, and the supernatant was filtered through a 0.22-μm syringe filter. The lysate was then passed through a HisTrap HP column (GE Healthcare, Piscataway, NJ, USA) that was equilibrated with Hepes buffer used for the cell lysis. The column was washed with 5–10 volumes of 20 mM Hepes buffer (pH 7.4) containing 300 mM NaCl and 68 mM imidazole. Protein was eluted with 20 mM Hepes (pH 7.4) containing 300 mM NaCl and 300 mM imidazole.

Plasma VWF and ADAMTS13

Multimeric human VWF was purified from plasma cryoprecipitate as described previously [19].

Recombinant human ADAMTS13 and diluted human plasma were used as a source of ADAMTS13 activity. To produce the recombinant protein, HEK 293T cells were transiently transfected with pCAGG-hADAMTS13 vector (a kind gift from Kenji Soejima, Chemo-Sero-Therapeutic Research Institute, Kaketsuken, Japan) using the calcium phosphate method [20]. After 8–12 h, culture medium was changed to chemically defined, serum-free medium Pro293a (Lonza, Basel, Switzerland) supplemented with GlutaMAX. Medium collected 48 h thereafter was concentrated 20-fold using Amicon 50-kDa cutoff centrifugal filter devices (Millipore) and dialyzed against 50 mM Tris (pH 8.0). In some cases, recombinant ADAMTS13 was also purchased from R&D Systems (Minneapolis, MN, USA). Human plasma was obtained from blood drawn from healthy nonsmoking volunteers into sodium citrate. All human subject protocols were approved by the University at Buffalo institutional review board. Platelet poor plasma (PPP) was obtained as described previously [19]. These samples were stored at −80 °C and thawed at 37 °C prior to use.

Proteolysis assays

Typically, FRET assays were performed in a 40-μl volume containing 1 μM VWF-A2 FRET protein and 8 μl of concentrated recombinant ADAMTS13 diluted in cleavage buffer (50 mM Tris [pH 8.0] and 12.5 mM $CaCl_2$). Urea was added to cleavage buffer in some cases. In other instances, protein was denatured with 4 M urea for 1 h at 37 °C prior to the addition of ADAMTS13. Comparison of FRETS-VWF73 (Peptides International, Louisville, KY, USA) and XS-VWF was performed in a 100-μl cleavage reaction mixture containing 1.5 μM substrate and 6 μl of plasma.

At fixed times, in some cases, VWF-A2 FRET fluorescence spectra were obtained using a spectrophotometer (model F-2500, Hitachi, Tokyo, Japan) with an excitation wavelength/slit width of 435/20 or 485/20 nm and an emission slit width of 5 nm. In other cases, proteolysis was quantified in 96/384-well black plates using a BioTek Synergy 4 or FLx800 reader (Winooski, VT, USA). These instruments were equipped with filters for Cerulean (excitation = 420/50 nm, emission = 485/20 nm) and Venus (excitation = 485/20 nm, emission = 540/25 nm). FRETS-VWF73 was read on the FLx800 reader equipped with 360/40-nm excitation and 460/40-nm emission filters. A parameter termed FRET ratio was used to quantify the extent of VWF-A2 FRET proteolysis. This is defined as the ratio of emitted light intensity at 485 nm (primarily by Cerulean) versus 540 nm (primarily by Venus) when the protein was excited at 420 nm. This parameter is inversely related to FRET efficiency, and it increases on VWF-A2 proteolysis.

Western blot analysis

Sodium dodecyl sulfate–polyacrylamide gel electrophoresis (SDS–PAGE) under standard reducing conditions was performed using either 4–20% gradient gels (Thermo Fisher, Rockford, IL, USA) for VWF-A2 FRET or 6% resolving gels for plasma VWF. Proteins were then transferred onto nitrocellulose membranes. These were detected using either goat anti-His polyclonal antibody (Bethyl Laboratories, Montgomery, TX, USA) for VWF-A2 FRET or rabbit anti-human VWF polyclonal antibody (Dako, Carpinteria, CA, USA) for plasma VWF. Silver staining was performed using a kit from Thermo Fisher.

Statistics

Unless stated otherwise, data are presented as mean ± standard errors of means for at least three replicate experiments. Analysis of variance (ANOVA) was applied for comparison between multiple treatments, and $P < 0.05$ was considered as significant.

Results

Truncated VWF-A2 constructs exhibit FRET properties

The entire VWF-A2 domain or fragments of this domain were engineered to express Venus at the N terminus and Cerulean at the C terminus (Fig. 1A). Although proteins with Citrine were also created, these were unsuitable for the current study because our emission spectra did not match earlier reports in the literature (see Supplementary Fig. S1 in supplementary material). All proteins with Venus and Cerulean were named based on the size of the inserted VWF-A2 fragment. Venus insertion sites were located in loop regions between β-sheets/α-helices based on X-ray crystal data [14] (Fig. 1B). Although the GFP variant insertion sites were located 77–175 amino acids from each other, in all proteins these sites are located within 2.5 nm in the crystal. Thus, the proteins were engineered to exhibit FRET properties. In addition, in the control protein, Y1605 and M1606 in the cleavage sequence in the smallest FRET construct (XS-VWF) both were mutated to alanine. All proteins were enriched using Ni-NTA (nitrilotriacetic acid) columns to more than 95% purity as assessed using silver staining of SDS–PAGE gels (Fig. 1C).

All proteins exhibited FRET properties (Fig. 2). FRET ratios varied from 0.74 for L-VWF to 1.24 for S-VWF. This corresponds to FRET efficiencies of 31% and 19%, respectively. Such variation is consistent with the notion that, in addition to the spatial distance separating the GFP variant insertion sites, the distance between these fluorophores in the fusion protein and their relative orientation also determine the energy transfer efficiency [21]. On the addition of ADAMTS13, FRET ratios increased from 0.78 to 1.73 for XS-VWF (Fig. 2A) and from 1.24 to 1.84 for S-VWF (Fig. 2B) within 1 h. Complete cleavage corresponds to a FRET ratio of approximately 2.2. There was very little change in the FRET ratio of M-VWF (Fig. 2C), L-VWF (Fig. 2D), or XS-VWF(AA) (Fig. 2E) on the addition of ADAMTS13. Western blot analysis of XS-VWF and XS-VWF(AA) (Fig. 2F) is consistent with the fluorescence measurements, and it confirms that changes in the FRET signal of XS-VWF are due primarily to the cleavage of the Y1605–M1606 scissile bond by ADAMTS13.

The K_M and k_{cat} values of XS-VWF and S-VWF were quantified based on a Lineweaver–Burk plot in the presence of 20% human plasma (Supplementary Fig. S2). These results show that both

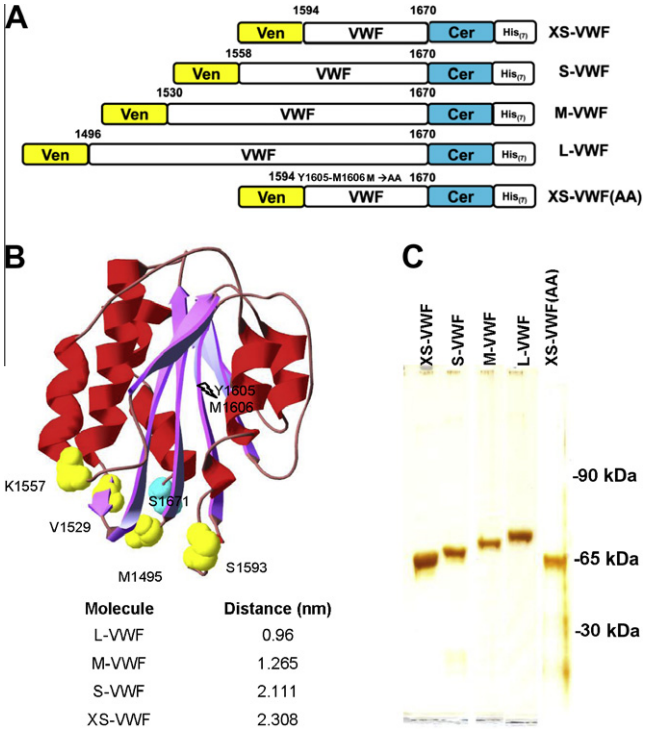

Fig.1. VWF-A2 FRET proteins. (A) Five FRET proteins were expressed and purified from *E. coli*. In these, Venus (Ven) and Cerulean (Cer) flank truncated fragments of the VWF-A2 domain. His tag is available for protein purification. The size of the A2 insertion increases from 77 amino acids for XS-VWF to 175 for L-VWF. XS-VWF(AA) is identical to XS-VWF except that the Y1605–M1606 amino acids in the ADAMTS13 cleavage site are replaced by A1605–A1606. (B) Relative positions of Cerulean (cyan) and Venus (yellow) in the family of FRET proteins are shown annotated in the VWF-A2 crystal (3GXB). Distances between Cerulean and Venus insertion sites in the crystal structure are listed. (C) Silver stain showing the purity of VWF-A2 FRET proteins. (For interpretation of the references to color in this figure legend, the reader is referred to the Web version of this article.)

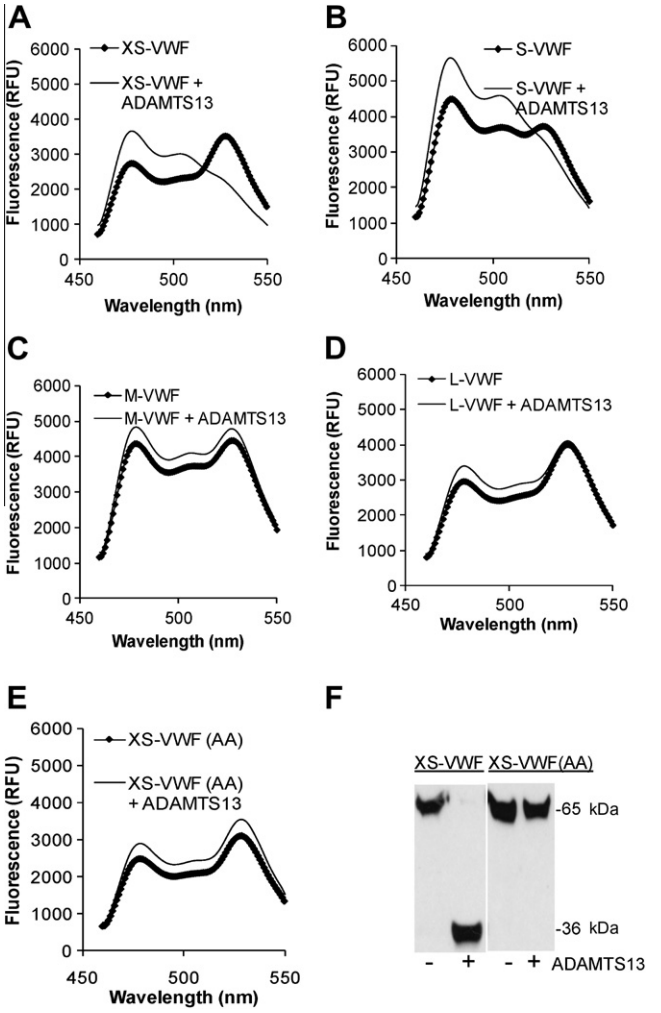

Fig.2. Fluorescence spectra and ADAMTS13 cleavage. Here 1 μM of each VWF-A2 FRET protein was incubated for 1 h at 37 °C either in the presence or in the absence of concentrated recombinant ADAMTS13. No denaturant was added. (A–E) Samples diluted 60-fold were analyzed using the fluorescence spectrophotometer with a 435-nm excitation wavelength. All spectra were normalized by arbitrarily setting YFP fluorescence intensity to 10,000 (excitation = 485 nm, emission = 530 nm). RFU, relative fluorescence units. (F) Selected samples at 1 h were subjected to Western blot analysis using anti-His polyclonal antibody for detection. XS-VWF, but not XS-VWF(AA), was cleaved by recombinant ADAMTS13. Data are representative of at least three experiments.

parameters were lower for S-VWF in comparison with XS-VWF (Table 2). Furthermore, the measured K_M and k_{cat} values were similar to previously published values for other proteins constructed based on the VWF-A2 domain.

Comparison of XS-VWF with FRETS-VWF73

We tested the ability of one of the VWF-A2 FRET proteins, XS-VWF, to detect ADAMTS13 activity in human plasma samples. On comparing cleavage rates of XS-VWF and FRETS-VWF73 using samples having a range of plasma ADAMTS13 activity and measured over time, we noted a linear change in the FRET ratio of XS-VWF with ADAMTS13 activity (Fig. 3A). Under identical conditions, FRETS-VWF73 fluorescence readout exhibited a nonlinear relationship with plasma ADAMTS13 activity (Fig. 3B).

When using normal human plasma, XS-VWF could be used to detect ADAMTS13 activity within 5 min, the earliest measured time point. In the presence of lower ADAMTS13 activity, more time was required for reliable detection of enzyme activity. Because autofluorescence due to plasma proteins plays only a minor role in assays using XS-VWF (Supplementary Fig. S3), higher plasma concentrations can be used for this substrate compared with FRETS-VWF73 that exhibits higher autofluorescence. When assays were performed by diluting 20 μl of a plasma mixture containing various ratios/amounts of normal plasma (100% ADAMTS13 activity) and heat-inactivated plasma (0% ADAMTS13 activity) in a 100-μl reaction volume, 10% of normal plasma protease activity could be detected within 30 min (Supplementary Fig. S4).

Table 2
Kinetic constants for the cleavage of different ADAMTS13 substrates.

Substrate	K_M	k_{cat} (min^{-1})	Reference
XS-VWF	4.6 ± 0.8 μM	44.8 ± 4.3	This study
S-VWF	1.8 ± 0.2 μM	17.7 ± 0.5	This study
FRETS-VWF73[a]	3.2 ± 1.1 μM	58	[39]
VWF115[b]	1.6 ± 0.5 μM	8.4 ± 3.6	[40]
Multimeric VWF	15 nM	0.83	[39]

[a] Substrate similar to XS-VWF.
[b] Substrate similar to S-VWF.

To further test our reagent, we compared substrate proteolysis with a panel of human plasma samples that were collected in sodium citrate (Table 3). The test samples included the following: (i) five calibration standards that had ADAMTS13 activity values assigned based on the dilutions of a pool of normal plasma collected by the International Society on Thrombosis and Haemostasis

(ISTH); (ii) proficiency specimens obtained from individuals deficient in ADAMTS13 activity (plasma sample 1), individuals with anti-ADAMTS13 antibodies (plasma sample 2), and normal controls (plasma sample 3) for these three samples, in some cases ADAMTS13 activity was heat-inactivated by incubating plasma at 56 °C for 30 min [specimens identified as "HI" in Table 3], whereas in other runs heat-inactivated plasma was mixed with an equal volume of normal plasma [identified as "mixed"] to check for anti-ADAMTS13 inhibitory antibodies [22]; (iii) six Factor Assay ConTrol (FACT) plasma samples from George King Biomedical (Overland Park, KS, USA) comprising two FACT plasma samples (11 and 12), two A-FACT plasma samples (5 and 6), and two B-FACT plasma samples (8 and 9) that exhibit normal, abnormal, and borderline activity in a wide variety of coagulation tests; and (iv) additional human plasma specimens exhibiting a range of ADAMTS13 activity levels (plasma samples 4, 7, and 10). As seen in Table 3, the results from XS-VWF activity measurements were largely consistent with findings noted using FRETS-VWF73. XS-VWF consistently gave lower values in the case of patients with less than 20% ADAMTS13 levels, whereas FRETS-VWF73 appears to overpredict this. This is particularly noted in the case of heat-inactivated plasma, with XS-VWF reporting values close to zero and FRETS-VWF73 reporting values of approximately 14%. Differences were also noted in some plasma samples, namely samples 5 and 6 and samples 8 and 9. The reason for this has not been identified, although it may be attributed to inherent structural differences in the two substrates and the manner in which ADAMTS13 binds them.

Table 3
XS-VWF versus FRETS-VWF73.

Sample	% Normal plasma ADAMTS13 activity	
	XS-VWF	FRETS-VWF73
CalA (AV = 0%)	−0.1 ± 0.14	−3.0 ± 0.7
CalB (AV = 11%)	8.3 ± 1.0	15.2 ± 1.4
CalC (AV = 31%)	32.9 ± 0.3	31.6 ± 0.7
CalD (AV = 64%)	66.7 ± 0.2	60.9 ± 0.0
CalE (AV = 107%)	104.8 ± 2.5	108.9 ± 0.3
Plasma 1	5.8 ± 0.2	22.9 ± 0.6
Plasma 1 (HI)	0.6 ± 1.0	18.6 ± 0.3
Plasma 1 (mixed)	46.7 ± 0.1	46.9 ± 0.1
Plasma 2	−3.2 ± 1.1	14.2 ± 1
Plasma 2 (HI)	−1.4 ± 1.2	13.4 ± 0.8
Plasma 2 (mixed)	−1.6 ± 1.2	16.2 ± 2.1
Plasma 3	103.2 ± 2.2	105.2 ± 3.0
Plasma 3 (HI)	−3.0 ± 1.4	9.6 ± 7.8
Plasma 3 (mixed)	48.9 ± 0.4	46.5 ± 1.1
Plasma 4	7.3 ± 1.8	12.4 ± 0.2
Plasma 5	25.8 ± 6.3	−1.6 ± 1.6
Plasma 6	21.0 ± 5.4	−4.6 ± 3.4
Plasma 7	24.9 ± 0.6	36.9 ± 1.6
Plasma 8	70.4 ± 14.9	32.1 ± 1.41
Plasma 9	67.4 ± 14.35	32.9 ± 1.3
Plasma 10	114.3 ± 23.4	80.7 ± 3.8
Plasma 11	116.0 ± 23.7	88.7 ± 2.1
Plasma 12	93.7 ± 0.4	80.9 ± 1.2

Note: ADAMTS13 activity was measured using either XS-VWF or FRETS-VWF73 as substrate for up to 45 min. Measured fluorescence value was converted to %ADAMTS13 activity using calibration curve in Fig. 3. Data from 30 and 45 min were averaged, and are presented as mean ± standard deviation. AV, activity value; HI, heat-inactivated.

Effect of urea on VWF-A2 folding and access to proteolysis site

Because ADAMTS13 alone could not cleave M- and L-VWF (Fig. 2), studies were performed where urea concentration in the cleavage buffer was varied from 0 to 3.2 M. Experiments were performed both in the absence (Fig. 4A) and in the presence (Fig. 4B and C) of ADAMTS13. In Fig. 4A, FRET ratios increased approximately linearly with urea concentrations even in the absence of ADAMTS13. Over this range of urea concentrations, there was negligible change in the fluorescence properties of Venus or Cerulean alone (data not shown). Significant structural changes occurred at urea concentrations down to 1.6 M.

ADAMTS13 was added to the VWF-A2 FRET proteins in the presence of varying urea concentrations. FRET ratio measurement (Fig. 4B) and Western blot analysis (Fig. 4C) of selected samples were performed. Complete cleavage of XS-VWF and S-VWF was observed at urea concentrations of less than 2.8 M. The data confirm that urea is not required for the cleavage of these proteins and that ADAMTS13 activity is diminished at high urea concentrations. In the absence of urea, the extent of cleavage of both L- and M-VWF was 20%. Increasing the urea concentration to 1.6 M resulted in 30% proteolysis. Complete proteolysis was not observed under any condition. Western blot analysis results (Fig. 4C) are consistent with the fluorescence measurements.

Because complete cleavage of L-VWF was not observed under any condition, we further increased the urea concentration by incubating L-VWF and multimeric human plasma VWF with 4 M urea for 1 h prior to dilution into a solution that contained ADAMTS13 along with lower urea concentrations (Fig. 5). Here we noted substantial cleavage of L-VWF even when the protein was diluted into buffer that lacked urea. More than 90% cleavage of L-VWF

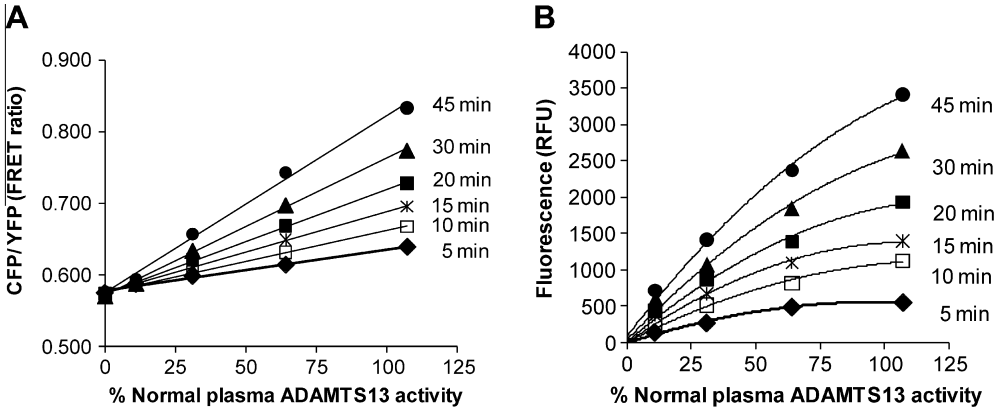

Fig.3. Detection of plasma ADAMTS13 levels by XS-VWF. Various dilutions of human plasma were incubated with 1.5 μM XS-VWF or FRETS-VWF73 under conditions optimized for the latter reagent. (A) FRET ratios varied linearly with plasma ADAMTS13 activity for XS-VWF. (B) FRETS-VWF73 fluorescence readouts varied nonlinearly with plasma ADAMTS13 activity. Data are representative of at least three experiments. RFU, relative fluorescence units.

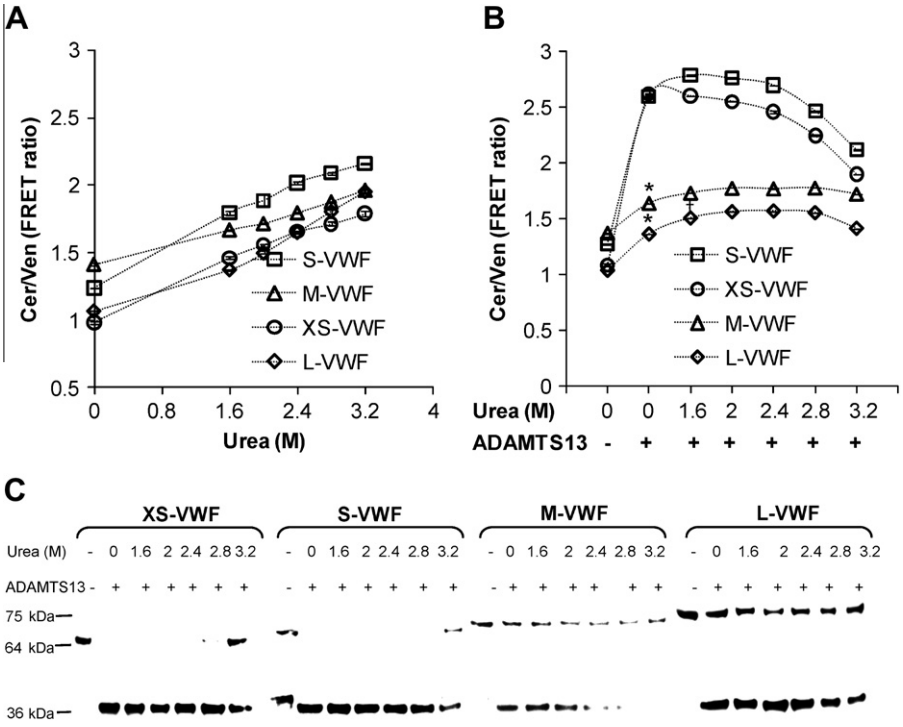

Fig.4. Effect of urea. (A) Here 2 μM of each VWF-A2 FRET protein was incubated with varying urea concentrations in the absence of ADAMTS13. FRET ratios, measured at 1 h, increased with urea concentration. (B) Concentrated recombinant ADAMTS13 was added to 1 μM VWF-A2 FRET proteins in the presence of varying urea concentrations for 2.5 h. Samples were then diluted in 20-fold excess buffer for an additional 5 min prior to FRET measurement. XS-VWF and S-VWF were cleaved efficiently in the absence of urea. The cleavage rate decreased at more than 2.4 M urea. The extent of L- and M-VWF cleavage increased with urea concentration, although neither substrate was fully cleaved in the available time. $^{*}P < 0.05$ with respect to sample without ADAMTS13; $^{\dagger}P < 0.05$ with respect to both samples that lack urea. (C) Western blot analysis of 3-h samples performed using the protocol in Fig. 2F is consistent with fluorescence data.

was observed at 2 M urea on inclusion of the predenaturation step (Fig. 5A and 5B). Similar to L-VWF, multimeric VWF was also not fully cleaved when the protein was incubated with varying urea concentrations and ADAMTS13 (Fig. 5C). However, proteolysis was complete at urea more than 2.4 M provided that a predenaturation step was included (Fig. 5D). This observation suggests that the proteolysis of L-VWF proceeds under similar denaturation conditions as the plasma protein.

Discussion

This article has described the family of VWF-A2 FRET proteins. Multiple lines of evidence suggest that the introduction of Venus and Cerulean in these molecules does not dramatically affect the function of these proteins. First, we observed that the addition of β-sheets at the N terminus increases the urea requirement for A2 cleavage. In this regard, whereas S- and XS-VWF are separated by α-helices and these were cleaved in the absence of urea, M-VWF includes the β_2- and β_3-sheets and L-VWF includes an additional β_1-sheet. This observation is consistent with the report by Kokame et al. [15], who applied Western blot analysis to study various truncated VWF fragments that lacked GFP variants. Whereas some protein needed to be refolded from inclusion bodies in that study [15] and this complicated interpretation, the molecules we produced were soluble. In addition to differences in the protein constructs used in the two studies, differences in the *E. coli* culture conditions may also contribute to enhanced protein solubility in our work. Second, the urea requirement for L-VWF proteolysis was similar to multimeric plasma VWF. In both cases, although some proteolysis was observed at more than 1.6 M urea, complete VWF-A2 proteolysis required denaturation using 4 M urea.

XS-VWF reports on plasma ADAMTS13 activity

XS-VWF can be used as a rapid, reliable, sensitive, and cost-effective reagent to monitor plasma ADAMTS13 activity. It can detect ADAMTS13 activity below 10% normal levels within 30 min. Such a reagent is important because it provides a measure of the hemostatic potential of blood. In addition to TTP, decreased ADAMTS13 activity is also associated with poor prognosis during sepsis-induced organ failure and with increased risk of nonfatal heart attack [11]. Reagents that detect ADAMTS13 activity can also be applied to distinguish TTP from other unrelated disorders such as hemolytic uremic syndrome (HUS) that present similar clinical symptoms [23,24].

Although several methodologies have been previously developed to assay for ADAMTS13 activity [25], XS-VWF provides some advantages. In comparison with traditional assays that monitor ultra-large VWF multimer distribution using Western blot analysis, results from XS-VWF are obtained more rapidly and are quantitative. As opposed to indirect measures of ADAMTS13 activity that monitor the binding of proteolytically cleaved patient/sample VWF to collagen in enzyme-linked immunosorbent assay (ELISA)-type assays [26], XS-VWF provides a more direct functional readout of enzyme activity. The experimental protocol is also less technically difficult to perform and is rapid. Thus, XS-VWF shares many of the advantages of the fluorogenic substrate FRETS-VWF73 [15,16]. In addition, XS-VWF is a recombinant protein that can likely be produced in a cost-effective manner. Under our assay conditions, it also exhibits a more linear relationship with plasma ADAMTS13 activity compared with FRETS-VWF73 and more reliably detects low levels of ADAMTS13 activity. Finally, XS-VWF uses higher excitation and emission wavelengths compared with FRETS-VWF73. This reduces the effects of autofluorescence due

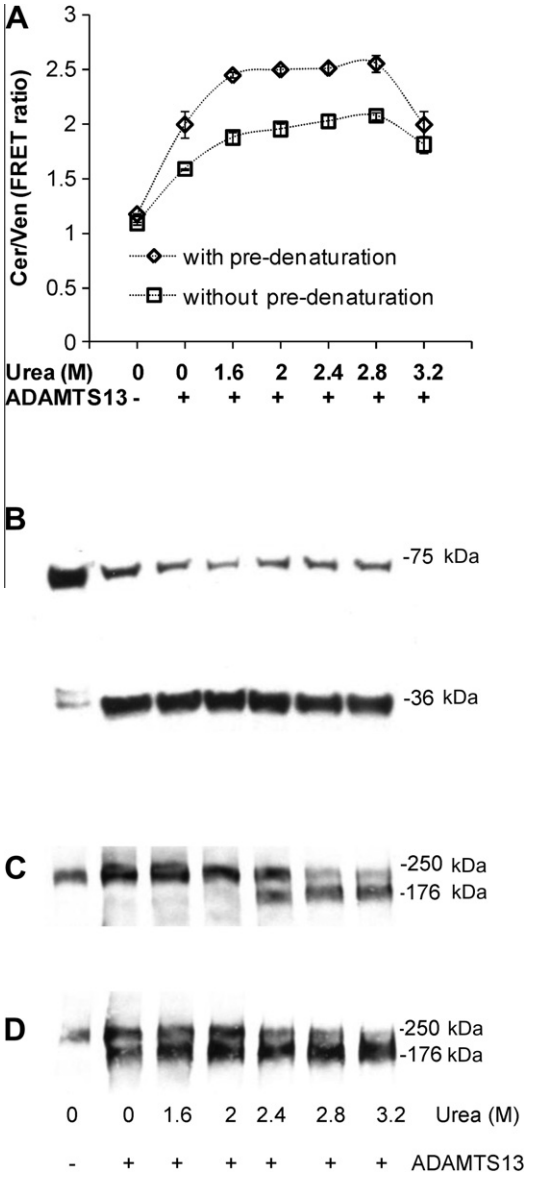

Fig.5. Predenaturation with urea. Here 10 μM L-VWF or 40 μg/ml multimeric plasma VWF was incubated either in the presence or in the absence of 4 M urea at 37 °C for 1 h. Following this, VWF samples were diluted 10-fold into cleavage buffer containing concentrated ADAMTS13 and varying urea amounts for 24 h. (A) The FRET ratio was measured similar to as in Fig. 4B. Predenaturation of L-VWF with 4 M urea enhanced proteolysis rates. (B) Western blot of L-VWF samples predenatured with urea prior to the addition of ADAMTS13 shows more than 90% proteolysis. (C and D) Western blot of plasma VWF that either was not subjected to (C) or was subjected to (D) urea predenaturation. Predenaturation is required for the efficient cleavage of both L-VWF and plasma VWF.

to plasma proteins. The use of higher wavelengths may also partially improve substrate performance in plasma samples having high levels of bilirubin because this yellow product quenches light with peak absorbance at 450 nm [27].

Although XS-VWF is likely to detect many instances of ADAMTS13 defect, the reagent has limitations because it lacks the additional domains of VWF. It is established that extensive molecular interaction between VWF and ADAMTS13 enables the proteolysis of the VWF-A2 domain. Exosites of ADAMTS13 bind sites in VWF are located both within and outside of the VWF-A2 domain. In this regard, based on X-ray crystallography and enzymatic investigations of the noncatalytic domains of ADAMTS13, it is suggested that multiple exosites located in the disintegrin-like (D), cysteine-rich (C), and spacer (S) domains of ADAMTS13 engage VWF-A2 [28]. The amino acids engaged by these exosites are located in the A2 domain between Pro1645 and Arg1668 [29]. In addition, Zanardelli et al. [30] suggested that VWF amino acids between the D4 and CK domains interact with the TSP5-CUB region of ADAMTS13. Mice lacking the TSP7-CUB at the C-terminal end of ADAMTS13 also exhibit reduced ADAMTS13 enzyme activity [31] and increased thrombus volume in regions of high shear stress [32]. Thus, although XS-VWF is likely to detect reduced activity of ADAMTS13 in most instances, it might not assay alterations in ADAMTS13 activity that are caused by mutations in enzyme exosite regions that engage domains other than the C-terminal section of VWF-A2. In addition, XS-VWF cannot be used in shear-based assays because the molecule is too small to "feel" the effect of hydrodynamic shear [9]. It also might not be effective in instances where plasma is contaminated with hemoglobin because this is reported to inhibit ADAMTS13 activity [33].

Progressive denaturation of VWF-A2 with urea concentration

Whereas the smallest FRET protein is well suited for measuring ADAMTS13 activity, the largest molecule (L-VWF) provides insight into the dynamics of VWF conformation change on the addition of denaturant. In this regard, others have used urea as a surrogate for fluid shear because this denaturant exposes the cryptic Y1605–M1606 cleavage site in VWF-A2 [34]. Our studies show that protein conformation changes progressively with urea concentration, consistent with the notion that multiple salt bridges stabilize the A2 domain. Alternatively, as shown for cold shock protein Csp*Tm*, chymotrypsin inhibitor 2 and other biomolecules [35,36], VWF-A2 FRET may exist in only a limited number of states, with urea regulating the distribution of the protein in these states. Additional single-molecule FRET studies over a wider range of denaturation conditions are necessary to determine the number of intermediate states that exist between fully folded and fully denatured VWF-A2.

In conclusion, the current study introduces new CFP/YFP-based FRET biosensors to measure VWF conformation change. Although the current proteins are expressed in *E. coli*, similar constructs can also be expressed in mammalian systems. CFP/YFP may also be incorporated into multimeric VWF to quantify structural changes in VWF due to hydrodynamic shear [10,37,38]. Such FRET-based proteins can be used to study the dynamics of VWF structural change under hydrodynamic shear, including the effects of protein glycosylation, *trans–cis* proline isomerization, and vicinal cysteines [14].

Acknowledgments

This work was supported by National Institutes of Health (NIH) grant HL 77258. We thank Elizabeth Wuitschick for technical assistance. XS-VWF is available from the corresponding author.

Appendix A. Supplementary data

Supplementary data associated with this article can be found, in the online version, at doi:10.1016/j.ab.2010.12.005.

References

[1] K. Fujikawa, H. Suzuki, B. McMullen, D. Chung, Purification of human von Willebrand factor-cleaving protease and its identification as a new member of the metalloproteinase family, Blood 98 (2001) 1662–1666.
[2] H.E. Gerritsen, R. Robles, B. Lammle, M. Furlan, Partial amino acid sequence of purified von Willebrand factor-cleaving protease, Blood 98 (2001) 1654–1661.
[3] K. Soejima, N. Mimura, M. Hirashima, H. Maeda, T. Hamamoto, T. Nakagaki, C. Nozaki, A novel human metalloprotease synthesized in the liver and secreted into the blood: possibly, the von Willebrand factor-cleaving protease? J. Biochem. 130 (2001) 475–480.

[4] H.M. Tsai, I.I. Sussman, R.L. Nagel, Shear stress enhances the proteolysis of von Willebrand factor in normal plasma, Blood 83 (1994) 2171–2179.
[5] K. Shim, P.J. Anderson, E.A. Tuley, E. Wiswall, J.E. Sadler, Platelet-VWF complexes are preferred substrates of ADAMTS13 under fluid shear stress, Blood 111 (2008) 651–657.
[6] J. Huang, R. Roth, J.E. Heuser, J.E. Sadler, Integrin $\alpha_v\beta_3$ on human endothelial cells binds von Willebrand factor strings under fluid shear stress, Blood 113 (2009) 1589–1597.
[7] R. Donadelli, J.N. Orje, C. Capoferri, G. Remuzzi, Z.M. Ruggeri, Size regulation of von Willebrand factor-mediated platelet thrombi by ADAMTS13 in flowing blood, Blood 107 (2006) 1943–1950.
[8] Y. Shida, K. Nishio, M. Sugimoto, T. Mizuno, M. Hamada, S. Kato, M. Matsumoto, K. Okuchi, Y. Fujimura, A. Yoshioka, Functional imaging of shear-dependent activity of ADAMTS13 in regulating mural thrombus growth under whole blood flow conditions, Blood 111 (2008) 1295–1298.
[9] H. Shankaran, S. Neelamegham, Hydrodynamic forces applied on intercellular bonds, soluble molecules, and cell-surface receptors, Biophys. J. 86 (2004) 576–588.
[10] K.M. Dayananda, I. Singh, N. Mondal, S. Neelamegham, von Willebrand factor self-association on platelet $GpIb_\alpha$ under hydrodynamic shear: effect on shear-induced platelet activation, Blood 116 (2010) 3990–3998.
[11] H.M. Tsai, Pathophysiology of thrombotic thrombocytopenic purpura, Int. J. Hematol. 91 (2010) 1–19.
[12] M.A. Rizzo, G.H. Springer, B. Granada, D.W. Piston, An improved cyan fluorescent protein variant useful for FRET, Nat. Biotechnol. 22 (2004) 445–449.
[13] T. Nagai, K. Ibata, E.S. Park, M. Kubota, K. Mikoshiba, A. Miyawaki, A variant of yellow fluorescent protein with fast and efficient maturation for cell-biological applications, Nat. Biotechnol. 20 (2002) 87–90.
[14] Q. Zhang, Y.F. Zhou, C.Z. Zhang, X. Zhang, C. Lu, T.A. Springer, Structural specializations of A2, a force-sensing domain in the ultralarge vascular protein von Willebrand factor, Proc. Natl. Acad. Sci. USA 106 (2009) 9226–9231.
[15] K. Kokame, M. Matsumoto, Y. Fujimura, T. Miyata, VWF73, a region from D1596 to R1668 of von Willebrand factor, provides a minimal substrate for ADAMTS-13, Blood 103 (2004) 607–612.
[16] K. Kokame, Y. Nobe, Y. Kokubo, A. Okayama, T. Miyata, FRETS-VWF73, a first fluorogenic substrate for ADAMTS13 assay, Br. J. Haematol. 129 (2005) 93–100.
[17] F. Peyvandi, R. Palla, L.A. Lotta, I. Mackie, M.A. Scully, S.J. Machin, ADAMTS-13 assays in thrombotic thrombocytopenic purpura, J. Thromb. Haemost. 8 (2010) 631–640.
[18] I. Singh, H. Shankaran, M.E. Beauharnois, Z. Xiao, P. Alexandridis, S. Neelamegham, Solution structure of human von Willebrand factor studied using small angle neutron scattering, J. Biol. Chem. 281 (2006) 38266–38275.
[19] H. Shankaran, P. Alexandridis, S. Neelamegham, Aspects of hydrodynamic shear regulating shear-induced platelet activation and self-association of von Willebrand factor in suspension, Blood 101 (2003) 2637–2645.
[20] K. Soejima, H. Nakamura, M. Hirashima, W. Morikawa, C. Nozaki, T. Nakagaki, Analysis on the molecular species and concentration of circulating ADAMTS13 in blood, J. Biochem. 139 (2006) 147–154.
[21] D.W. Piston, G.J. Kremers, Fluorescent protein FRET: the good, the bad, and the ugly, Trends Biochem. Sci. 32 (2007) 407–414.
[22] H.M. Tsai, E.C. Lian, Antibodies to von Willebrand factor-cleaving protease in acute thrombotic thrombocytopenic purpura, N. Engl. J. Med. 339 (1998) 1585–1594.
[23] B.R. Forzley, W.F. Clark, TTP/HUS and prognosis: the syndrome and the disease(s), Kidney Int. Suppl. (2009) S59–S61.
[24] M.B. Marques, Thrombotic thrombocytopenic purpura and heparin-induced thrombocytopenia: two unique causes of life-threatening thrombocytopenia, Clin. Lab. Med. 29 (2009) 321–338.
[25] A. Tripodi, F. Peyvandi, V. Chantarangkul, R. Palla, A. Afrasiabi, M.T. Canciani, D.W. Chung, S. Ferrari, Y. Fujimura, M. Karimi, K. Kokame, J.A. Kremer Hovinga, B. Lammle, S.F. de Meyer, B. Plaimauer, K. Vanhoorelbeke, K. Varadi, P.M. Mannucci, Second international collaborative study evaluating performance characteristics of methods measuring the von Willebrand factor cleaving protease (ADAMTS-13), J. Thromb. Haemost. 6 (2008) 1534–1541.
[26] H.E. Gerritsen, P.L. Turecek, H.P. Schwarz, B. Lammle, M. Furlan, Assay of von Willebrand factor (vWF)-cleaving protease based on decreased collagen binding affinity of degraded vWF: a tool for the diagnosis of thrombotic thrombocytopenic purpura (TTP), Thromb. Haemost. 82 (1999) 1386–1389.
[27] S.C. Meyer, I. Sulzer, B. Lämmle, J.A. Kremer Hovinga, Hyperbilirubinemia interferes with ADAMTS-13 activity measurement by FRETS-VWF73 assay: diagnostic relevance in patients suffering from acute thrombotic microangiopathies, J. Thromb. Haemost. 5 (2007) 866–867.
[28] M. Akiyama, S. Takeda, K. Kokame, J. Takagi, T. Miyata, Crystal structures of the noncatalytic domains of ADAMTS13 reveal multiple discontinuous exosites for von Willebrand factor, Proc. Natl. Acad. Sci. USA 106 (2009) 19274–19279.
[29] J.J. Wu, K. Fujikawa, B.A. McMullen, D.W. Chung, Characterization of a core binding site for ADAMTS-13 in the A2 domain of von Willebrand factor, Proc. Natl. Acad. Sci. USA 103 (2006) 18470–18474.
[30] S. Zanardelli, A.C. Chion, E. Groot, P.J. Lenting, T.A. McKinnon, M.A. Laffan, M. Tseng, D.A. Lane, A novel binding site for ADAMTS13 constitutively exposed on the surface of globular VWF, Blood 114 (2009) 2819–2828.
[31] W. Zhou, E.E. Bouhassira, H.M. Tsai, An IAP retrotransposon in the mouse ADAMTS13 gene creates ADAMTS13 variant proteins that are less effective in cleaving von Willebrand factor multimers, Blood 110 (2007) 886–893.
[32] F. Banno, A.K. Chauhan, K. Kokame, J. Yang, S. Miyata, D.D. Wagner, T. Miyata, The distal carboxyl-terminal domains of ADAMTS13 are required for regulation of in vivo thrombus formation, Blood 113 (2009) 5323–5329.
[33] J.D. Studt, J.A. Hovinga, G. Antoine, M. Hermann, M. Rieger, F. Scheiflinger, B. Lammle, Fatal congenital thrombotic thrombocytopenic purpura with apparent ADAMTS13 inhibitor: in vitro inhibition of ADAMTS13 activity by hemoglobin, Blood 105 (2005) 542–544.
[34] M. Auton, M.A. Cruz, J. Moake, Conformational stability and domain unfolding of the von Willebrand factor A domains, J. Mol. Biol. 366 (2007) 986–1000.
[35] B. Schuler, W.A. Eaton, Protein folding studied by single-molecule FRET, Curr. Opin. Struct. Biol. 18 (2008) 16–26.
[36] A. Borgia, P.M. Williams, J. Clarke, Single-molecule studies of protein folding, Annu. Rev. Biochem. 77 (2008) 101–125.
[37] I. Singh, E. Themistou, L. Porcar, S. Neelamegham, Fluid shear induces conformation change in human blood protein von Willebrand factor in solution, Biophys. J. 96 (2009) 2313–2320.
[38] E. Themistou, I. Singh, C. Shang, S.V. Balu-Iyer, P. Alexandridis, S. Neelamegham, Application of fluorescence spectroscopy to quantify shear-induced protein conformation change, Biophys. J. 97 (2009) 2567–2576.
[39] P.J. Anderson, K. Kokame, J.E. Sadler, Zinc and calcium ions cooperatively modulate ADAMTS13 activity, J. Biol. Chem. 281 (2006) 850–857.
[40] S. Zanardelli, J.T. Crawley, C.K. Chion, J.K. Lam, R.J. Preston, D.A. Lane, ADAMTS13 substrate recognition of von Willebrand factor A2 domain, J. Biol. Chem. 281 (2006) 1555–1563.